

Statistical mechanical approach of complex networks with weighted links

Rute Oliveira,¹ Samuráí Brito,^{2,3} Luciano R. da Silva,^{1,4} and Constantino Tsallis^{4,5,6,7}

¹*Federal University of Rio Grande do Norte, Departamento de Física Teórica e Experimental, Natal-RN, 59078-900, Brazil.*

²*Emerging Technology Group at Itau-Unibanco*

³*International Institute of Physics, Federal University of Rio Grande do Norte, 59070-405 Natal, Brazil*

⁴*National Institute of Science and Technology of Complex Systems, Brazil.*

⁵*Centro Brasileiro de Pesquisas Físicas, Rua Xavier Sigaud 150, 22290-180 Rio de Janeiro-RJ, Brazil.*

⁶*Santa Fe Institute, 1399 Hyde Park Road, New Mexico 87501, USA*

⁷*Complexity Science Hub Vienna, Josefstaedter Strasse 39, A 1080 Vienna, Austria.*

(Dated: December 22, 2021)

Systems which consist of many localized constituents interacting with each other can be represented by complex networks. Consistently, network science has become highly popular in vast fields focusing on natural, artificial and social systems. We numerically analyze the growth of d -dimensional geographic networks (characterized by the index $\alpha_G \geq 0$; $d = 1, 2, 3, 4$) whose links are weighted through a predefined random probability distribution, namely $P(w) \propto e^{-|w-w_c|/\tau}$, w being the weight ($w_c \geq 0$; $\tau > 0$). In this model, each site has an evolving degree k_i and a local energy $\varepsilon_i \equiv \sum_{j=1}^{k_i} w_{ij}/2$ ($i = 1, 2, \dots, N$) that depend on the weights of the links connected to it. Each newly arriving site links to one of the pre-existing ones through preferential attachment given by the probability $\Pi_{ij} \propto \varepsilon_i/d_{ij}^{\alpha_A}$ ($\alpha_A \geq 0$), where d_{ij} is the Euclidean distance between the sites. Short- and long-range interactions respectively correspond to $\alpha_A/d > 1$ and $0 \leq \alpha_A/d \leq 1$; $\alpha_A/d \rightarrow \infty$ corresponds to interactions between close neighbors, and $\alpha_A/d \rightarrow 0$ corresponds to infinitely-ranged interactions. The site energy distribution $p(\varepsilon)$ corresponds to the usual degree distribution $p(k)$ as the particular instance $(w_c, \tau) = (2, 0)$. We numerically verify that the corresponding connectivity distribution $p(\varepsilon)$ converges, when $\alpha_A/d \rightarrow \infty$, to the weight distribution $P(w)$ for infinitely narrow distributions (i.e., $\tau \rightarrow \infty, \forall w_c$) as well as for $w_c \rightarrow 0, \forall \tau$. Finally, we show that $p(\varepsilon)$ is well approached by the q -exponential distribution $e_q^{-\beta_q |\varepsilon - w_c|}$ [$0 \leq w'_c(w_c, \alpha_A/d) \leq w_c$] which optimizes the nonadditive entropy S_q under simple constraints; q depends only on α_A/d , thus exhibiting universality.

I. INTRODUCTION

Network science is extremely effective in studying large interacting systems. Within this approach, systems are described by graphs, with nodes (or sites) representing the individual components and edges (or links) representing the interactions between them. Empirical studies show that complex networks are ubiquitous [1–3]. It has been possible, along such lines, to understand the propagation of information [4, 5], classical and quantum internet connections [6, 7], scientific collaborations [8, 9], epidemiology [10, 11], and human brain [12]. Consistently, in recent decades, mathematical models have emerged to mimic real systems and reproduce their structural properties [13]. In Euclidean space, geographical networks have also been studied, such as subway systems [14], neural [15], internet and transportation networks [16]. Also, many real world networks are weighted by assigning real numbers to their edges [17]. For example, the US air transportation network [18], where the weights of the edges represent the total number of passengers.

Statistical mechanics is intensively used to study systems with complex geometric and topological properties. In many such systems, the elements exhibit long-

range interactions [19]. To handle these cases, a generalization of the Boltzmann–Gibbs (BG) statistical mechanics was proposed in 1988 [20], currently referred to as nonextensive statistical mechanics, based on the nonadditive entropies $S_q = k \frac{1 - \sum_i p_i^q}{q-1}$ with $q \in \mathbb{R}$. The BG theory is recovered for $q \rightarrow 1$. This generalized approach has been applied in a large variety of systems, e.g., spin-glasses [21], astrophysical plasma [22], urban agglomerations [23], velocities of collective migrating cells [24], cold atoms in dissipative optical lattices [25, 26], among others.

The relationship between asymptotically scale-free d -dimensional geographic networks and nonextensive statistical mechanics started being explored in 2005 [27–32], where a preferential attachment index α_A and a growth index α_G were included. These studies showed that geographic networks exhibit three regimes: (a) $0 \leq \alpha_A/d \leq 1$, corresponding to strongly long-range interactions, (b) $1 \leq \alpha_A/d \lesssim 5$, corresponding to moderately long-range interactions, and (c) $\alpha_A/d \gtrsim 5$, corresponding to the BG-like regime, i.e., $q \simeq 1$ (short-range interactions).

In a recent study, we have introduced a d -dimensional geographical network with weighted links [32] where we use a stretched-exponential distribution $P(w)$ for the

weight w . We analyzed the distribution of site 'energies' (or costs) $p(\varepsilon)$, where

$$\varepsilon_i \equiv \sum_{j=1}^{k_i} \frac{w_{ij}}{2}, \quad (1)$$

k_i being the degree of the i -th site; the factor $1/2$ is introduced to avoid double counting. We verified that $p(\varepsilon)$ is numerically very close to $p_q(\varepsilon) \equiv e_q^{-\beta_q \varepsilon} / Z_q$, where $p_q(\varepsilon)$ generalizes the BG factor, β_q playing the role of an inverse temperature and Z_q being the normalization factor; the q -exponential function is defined as $e_q^z \equiv [1 + (q-1)z]^{\frac{1}{1-q}}$ ($e_1^z = e^z$). We also showed that q exhibits a universal behaviour, depending only on the scaled variable α_A/d .

Our aim here is to study the energy distribution $p(\varepsilon)$ corresponding to a Laplace-like weight distribution. In particular, we compare $p(\varepsilon)$ with $P(w)$ and with the q -exponential form.

The comparison of distributions is common in diverse scenarios. From algorithms to generate pseudo-random numbers [33], through the validity of empirical data with regard to the corresponding theoretical distribution [34, 35] and the identification of images [36, 37], to distributions of aquatic organisms [38]. Interestingly enough, the studies [39, 40] show that the site energy (total weight) distribution converges (excepting for a logarithmic correction) to the scaling behavior of the connectivity (or degree) distribution of the network. Empirical studies exhibit some real-world examples of networks where this phenomenon or similar ones have been observed, e.g., in book borrowing, movie actor collaborations [40], worldwide airport connections, scientific collaborations [41], and others. In the present work we numerically show that, when $(\tau \rightarrow \infty, \forall w_c)$ and $(w_c \rightarrow 0, \forall \tau)$, the energy distribution $p(\varepsilon)$ and the weight distribution $P(w)$ become identical in the regime of short-range interactions ($\alpha_A/d \gg 1$).

The paper is structured as follows. In Sec. II we describe our network model, including the weight distribution and its stochastic implementation. In Sec. III we analyze the numerical energy distribution and compare it with the weight distribution of the links, as well as with the q -exponential form emerging from optimizing the nonadditive entropy S_q . Finally, in Sec. IV we conclude.

II. THE MODEL

Our network model starts with one site at the origin and then, for each new site added to the network, we randomly sample a position for it according to the isotropic distribution $p(r) \propto 1/r^{d+\alpha_G}$ ($\alpha_G > 0$; $d = 1, 2, 3, 4$), where $r \geq 1$ is the Euclidean distance

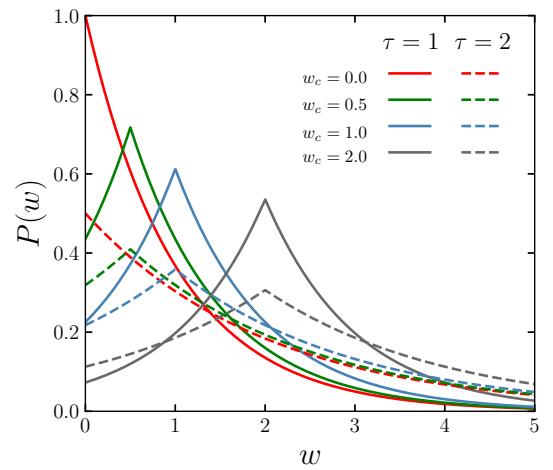


FIG. 1. Weight distribution curves for $\tau = 1$ (continuous lines) and $\tau = 2$ (dashed-dotted lines), for typical values of w_c .

from the center of mass to the new site, and α_G is the growth index. Then, we link every newly arriving site (j) to one of the pre-existing ones in the network according to the following preferential attachment rule:

$$\Pi_{ij} = \frac{\varepsilon_i d_{ij}^{-\alpha_A}}{\sum_k \varepsilon_k d_{kj}^{-\alpha_A}} \in [0, 1] \quad (\alpha_A \geq 0), \quad (2)$$

where d_{ij} is the Euclidean distance between sites i and j and the attachment index α_A characterizes the range of the interactions; when $\alpha_A \rightarrow 0$ the system has long-range interactions and the distance loses relevance, whereas for $\alpha_A \rightarrow \infty$ the sites have short-range interactions (connections between close neighbors). To each site of the network we associate, through Eq. (1), a local energy ε_i which depends on the number of links.

In the present paper, we are using the following Laplace-like distribution (see Fig. 1) for the weights of the links:

$$P(w) = \frac{1}{2\tau - \tau e^{-w_c/\tau}} e^{-|w-w_c|/\tau} \quad (w_c \geq 0; \tau > 0), \quad (3)$$

which satisfies $\int_0^\infty P(w) = 1$, τ characterizing the distribution width and w_c being the location parameter. To numerically get values of the variable w from this distribution we use the inverse transformation method [42]:

$$w = w_c - \text{sgn} \left[u - A\tau(1 - e^{-w_c/\tau}) \right] \tau \ln \left\{ 1 + \text{sgn} \left[u - A\tau(1 - e^{-w_c/\tau}) \right] \left[1 - (u/A\tau + e^{-w_c/\tau}) \right] \right\}, \quad (4)$$

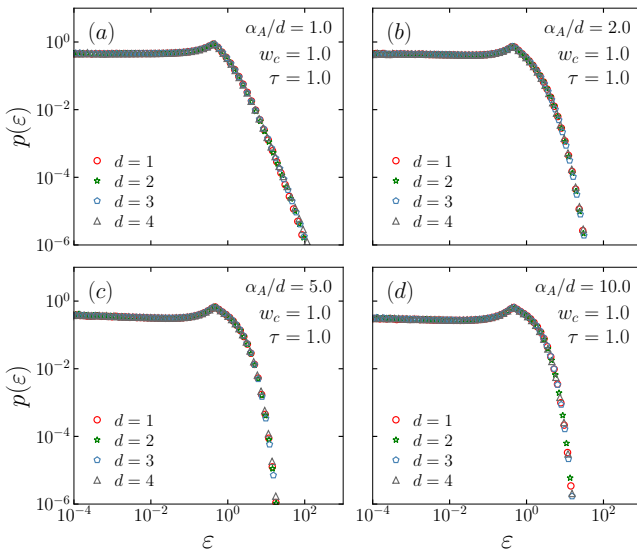


FIG. 2. Local energy distribution $p(\varepsilon)$ for typical values of $d = 1, 2, 3, 4$ with (a) $\alpha_A/d = 1$, (b) $\alpha_A/d = 2$, (c) $\alpha_A/d = 5$ and (d) $\alpha_A/d = 10$, with $(\alpha_G, \tau, w_c) = (1, 1, 1)$. The simulations are averaged over 10^3 realisations for $N = 10^5$ sites.

where $A = 1/(2\tau - \tau e^{-w_c/\tau})$ is the normalization constant [see Eq. (3)], u is a uniform random variable between $[0, 1]$ and $\text{sgn}(\theta)$ denotes the sign function:

$$\text{sgn}(\theta) = \begin{cases} -1, & \text{if } \theta < 0, \\ 0, & \text{if } \theta = 0, \\ 1, & \text{if } \theta > 0. \end{cases}$$

III. SIMULATIONS AND RESULTS

We now focus on the energy distribution $p(\varepsilon)$ and compare it with the weight distribution of the links $P(w)$. The weight distribution has two free parameters, namely τ and w_c , while our model has three parameters, namely α_A , α_G and d , in addition to the weight distribution itself. We fix these parameters and numerically determine $p(\varepsilon)$ by using a large number N of sites (typically $N = 10^5$) and performing a large number of realizations (typically 10^3).

We verify that the energy distribution is completely independent from α_G in all situations, as already discussed in earlier publications [27–30, 32]. Consequently, we fix it to be $\alpha_G = 1$ in all our simulations. Also, we observe that $p(\varepsilon)$ remains invariant when we fix α_A/d and we modify the values of $d = 1, 2, 3, 4$, as shown in Fig. 2. This implies an universality property, namely that the energy distribution depends on the ratio α_A/d and does not depend independently on α_A and

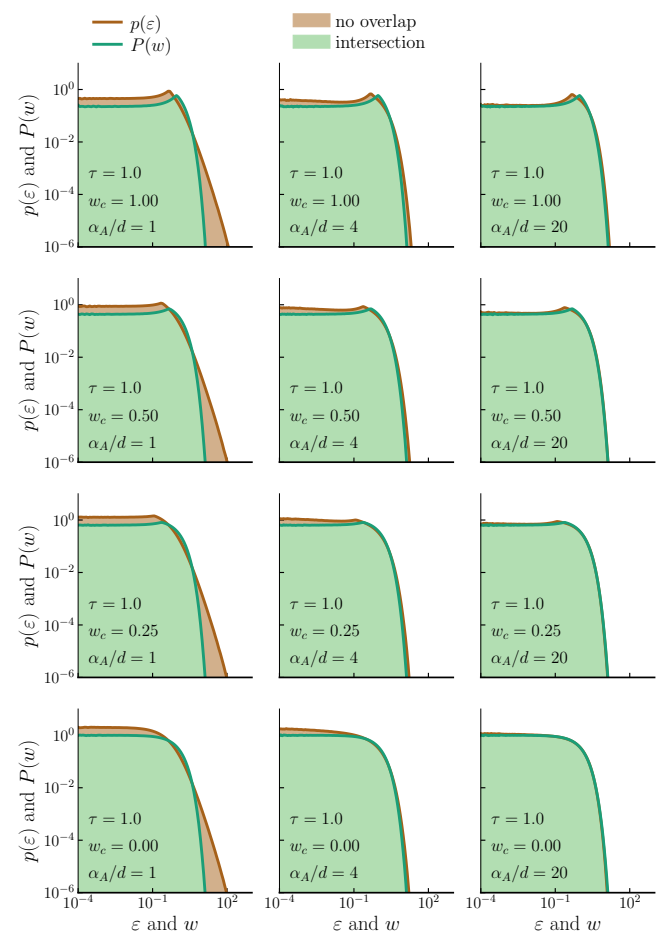


FIG. 3. The simulations are carried out for typical values of $w_c = (1, 0.50, 0.25, 0.00)$ and $\alpha_A/d = (1, 4, 20)$ with $\tau = 1$. The green continuous lines correspond to the weight distribution, given by Eq. (3), and the brown continuous lines correspond to the energy distribution. The green area is the region of intersection and the brown area denotes the region where the weight and energy distributions do not intersect. The simulations are averaged over 10^3 realisations for $N = 10^5$ sites.

on d [28–32]. In consequence, we present our results by simply running $d = 2$.

We choose typical values for the parameter $\tau = 1$ and 10, and for the location parameter $w_c = 0, 0.25, 0.5, 1$ and 2, and generate networks for fixed values of the attachment parameter α_A . We compare the weight and the energy distributions through their histograms by using a function from the Python Library Numpy [43]. This function has some input parameters (array, bins, density, etc.) and returns the probability density function at each bin (with n bins in total, b_1, \dots, b_n) where the integral over the entire interval equals unity.

There are many methods in the literature for comparing histograms. We use here two of them, namely Histogram Intersection [36] and Q-Q (quantile-quantile)

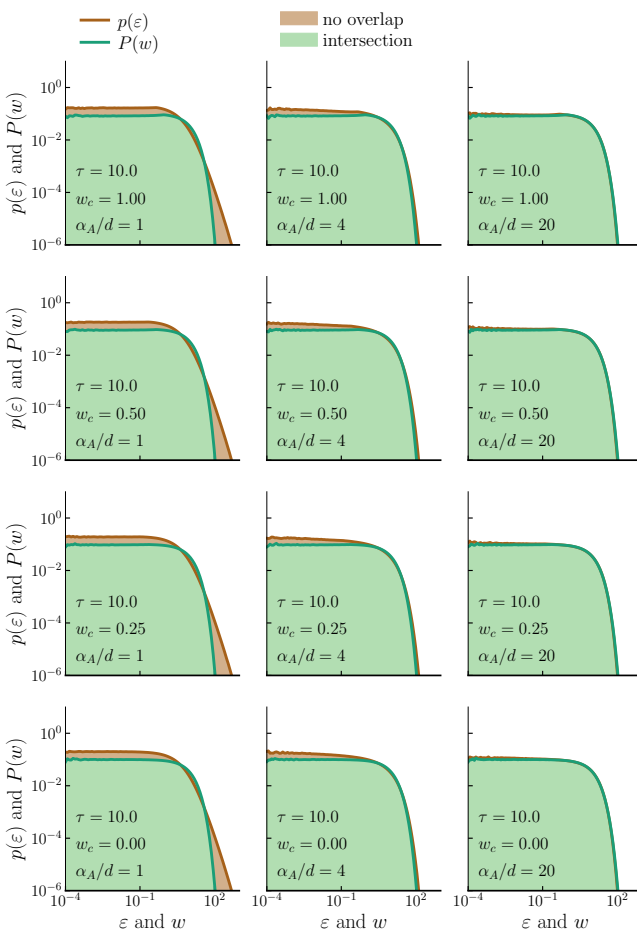


FIG. 4. The same as in Fig. 3 but with $\tau = 10$.

plot, to compare $p(\varepsilon)$ and $P(w)$. The histogram intersection method is a technique used for image indexing and comparison, where the image colors are discretized by a histogram and compared to a original figure. Given two histograms, H_w and H_ε , containing the same number n of bins, Swain and Ballard [36] defined the histogram intersection as the sum of the minima for all histogram bins:

$$H_w \cap H_\varepsilon = \sum_{i=1}^n \min [h_w(i), h_\varepsilon(i)], \quad (5)$$

the range of this calculus goes from 0 to 1, where 0 indicates that the histograms do not intersect at all and 1 means that the histograms are identical.

In Figs. 3 and 4 we show the energy and weight distributions for $\tau = 1$ and $\tau = 10$ respectively. We observe that when $\alpha_A/d \sim 1$ the histograms are sensibly different, whereas when α_A/d increases they become quite similar. In the limit $\alpha_A/d \rightarrow \infty$, the distributions are practically identical. This behaviour is shown in Fig. 5.

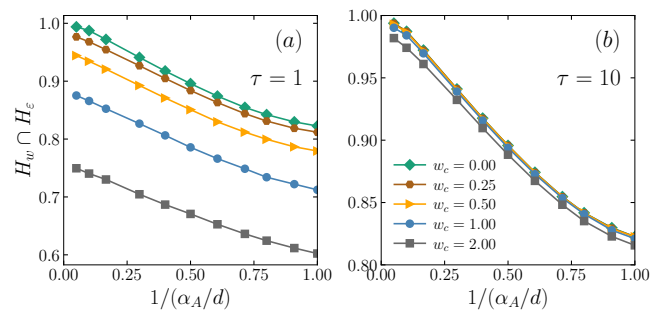


FIG. 5. $H_w \cap H_\varepsilon$ versus $1/(\alpha_A/d)$ for (a) $\tau = 1$ and (b) $\tau = 10$. We see that $H_w \cap H_\varepsilon \rightarrow 1$ for $1/(\alpha_A/d) \rightarrow 0$ when $w_c \rightarrow 0$ ($\forall \tau$).

TABLE I. Values used for β_{q_0} and β_{q_∞} in Eq. (9). The parameters β_{q_0} and β_{q_∞} correspond to $\alpha_A/d = 1$ and $\alpha_A/d = 20$ respectively. These results are for $N = 10^5$ sites averaged over 10^3 realizations.

w_c	β_{q_0}	β_{q_∞}
0.00	3.33	1.14
0.25	2.80	1.04
0.50	2.55	1.00

This result is more pronounced when $w_c \rightarrow 0$.

Alternatively, we can also recover the same results through the quantile probability plot (Q-Q plot), which is a graphical method for comparing two probability distributions by plotting the quantile of the first distribution against the same quantile of the second one. If $F(x)$ is a distribution function, the p^{th} quantile of F is defined as [44]:

$$\xi_p \equiv \inf\{x : F(x) \leq p\} \quad (0 < p < 1). \quad (6)$$

If the two distributions are very close then the points in the Q-Q plot will fall approximately along a straight line, namely the bisector: see Fig. 6, where $p(\varepsilon)$ and $P(w)$ are compared.

Let us now compare $p(\varepsilon)$ with the following q -exponential form:

$$p_q(\varepsilon) = \frac{e_q^{-\beta_q |\varepsilon - w'_c|}}{Z_q}, \quad (7)$$

where $w'_c \in [0, w_c]$ is a location parameter playing the role of a chemical potential in $p_q(\varepsilon)$, q is the entropic index, β_q playing the role of an inverse temperature, and Z_q is the normalization factor (see Fig. 7a-c). The particular case $w_c = 0$ corresponds to an exponential distribution and we recover the results obtained in our previous study [32], where we used the stretched-exponential distribution for the link weight $P(w) \propto e^{-(w/w_0)^\eta}$ for $\eta = 1$.

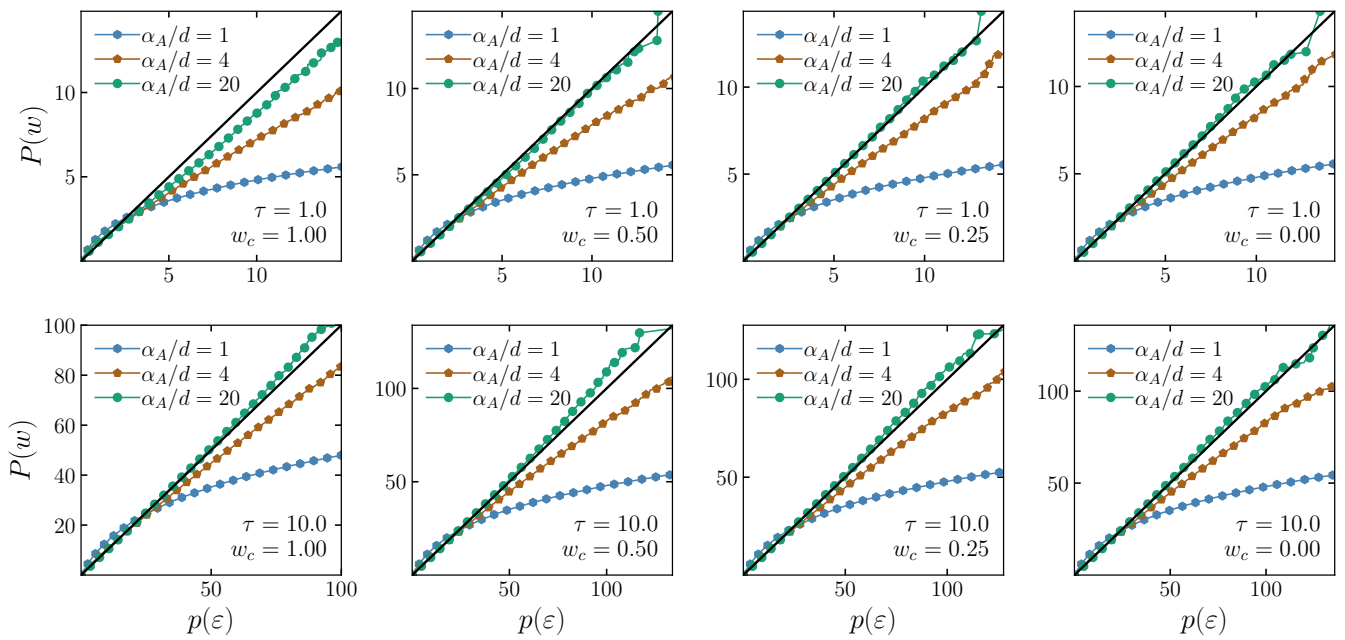


FIG. 6. Q-Q plot for $\tau = 1$ (top) and $\tau = 10$ (bottom), and typical values of $\alpha_A/d = 1$ (blue diamond), 4 (brown hexagon), 20 (green circle). In all cases the black continuous line corresponds to the bisector. The simulations were averaged over 800 realisations for $N = 10^5$ sites.

In Fig. 7(d-f) we exhibit the variables q , β_q and w'_c as functions of the ratio α_A/d . We numerically show that q only depends on this ratio; β_q also depends on w_c . Interestingly enough, both variables are given by the same equations indicated in [32], i. e.,

$$q = \begin{cases} \frac{4}{3} & \text{if } 0 \leq \frac{\alpha_A}{d} \leq 1 \\ \frac{1}{3} e^{1-\alpha_A/d} + 1 & \text{if } \frac{\alpha_A}{d} > 1 \end{cases} \quad (8)$$

and

$$\tau \beta_q = \begin{cases} \beta_{q0} & \text{if } 0 \leq \frac{\alpha_A}{d} \leq 1 \\ (\beta_{q0} - \beta_{q\infty}) e^{2(1-\alpha_A/d)} + \beta_{q\infty} & \text{if } \frac{\alpha_A}{d} > 1, \end{cases} \quad (9)$$

where the variables β_{q0} and $\beta_{q\infty}$ are listed in Table I. In all cases we observe the existence of three regimes, consistent with [28, 30, 32]. For $0 \leq \alpha_A/d \leq 1$, q , β_q and w'_c are constants, the system presenting very-long-range interactions. For $1 < \alpha_A/d \lesssim 5$, the system exhibits moderately-long-range interactions, where q and β_q monotonically decrease with α_A/d , whereas w'_c increases. In the limit of $\alpha_A/d \rightarrow \infty$, the parameters tend to constant values and this regime corresponds to short-range interactions ($q \rightarrow 1$).

IV. CONCLUSIONS

Many real systems contain sites whose importance (here denoted as *energy*) is generated by interactions

with the other sites through weighted links. This is the kind of situation that our network model mimics. Our simulations yield energy distributions which depend on α_A and on d through the ratio α_A/d . Indeed, the results collapse into a single curve for any spacial dimension. In addition to that, $p(\varepsilon)$ does not depend on α_G . We have also shown that, in the regime of short-range interactions ($\alpha_A/d \rightarrow \infty$), the energy distribution coincides with the weight distribution. Based on the intersection of the histograms of those two distributions, and also on the quantile-quantile plot, we have provided strong numerical evidence that this is indeed so for the distribution given in Eq. (3). It might well be that this result is more general than here verified, i.e., the same result might be true for other distributions $P(w)$.

We have also shown that the energy distribution $p(\varepsilon)$ is well approached by the form $e_q^{-\beta_q |\varepsilon - w'_c|}$, where e_q^x is the q -exponential function emerging within q -statistics [20], β_q playing the role of an inverse temperature. It is quite remarkable that the (α_A/d) -dependence of q precisely coincides with that obtained in [32] for a different distribution $P(w)$. This reinforces the strength of an universality conjecture concerning the entropic index q . In particular, Eqs. (8) and (9) appear to have a quite generic validity.

Let us conclude by a rather general comment. Various examples are known where Boltzmann-Gibbs statistical mechanical systems are isomorphic to random

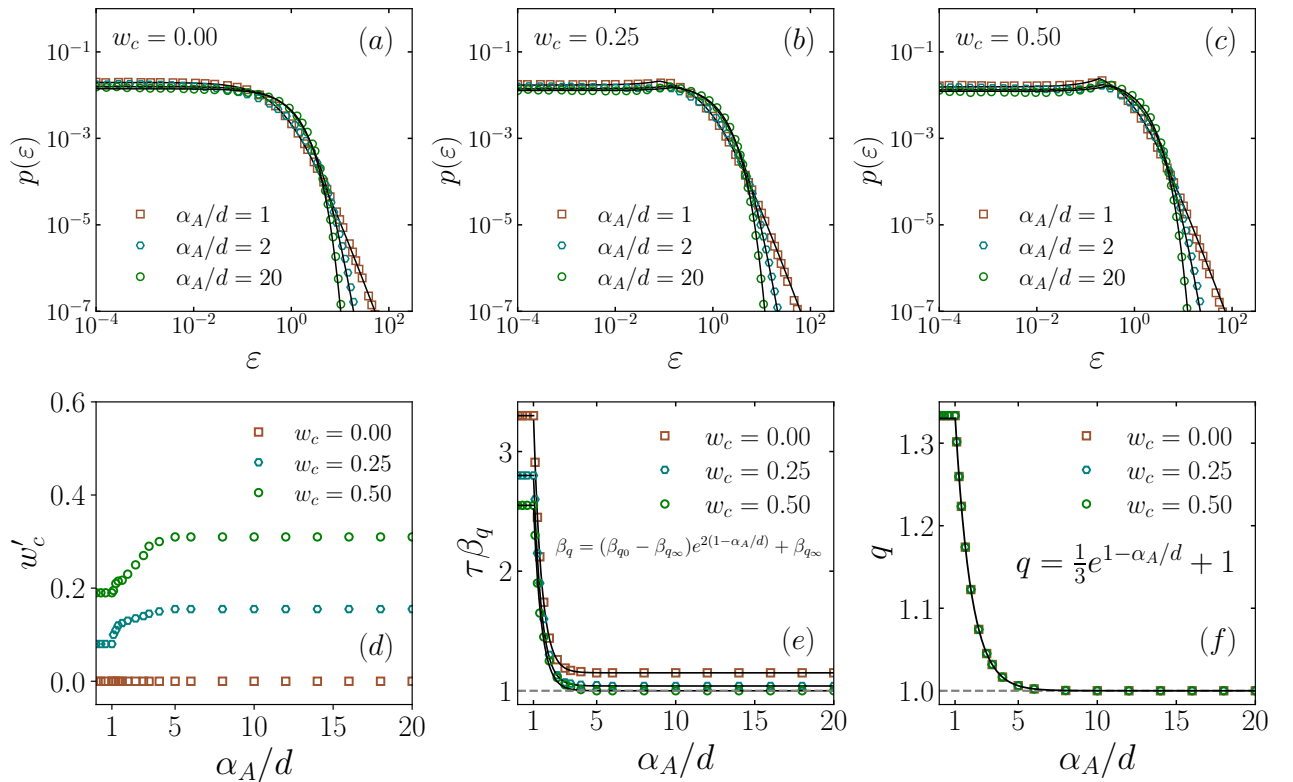


FIG. 7. Top: Energy distribution for $w_c = 0.00$ (a), $w_c = 0.25$ (b) and $w_c = 0.50$ (c), and $\alpha_A/d = 1, 2, 20$, with $\tau = 1$. The black continuous lines correspond to Eq. (7) with q and β_q given by Eqs. (8) and (9) respectively. Bottom: (d) w'_c as function of α_A/d for typical values of w_c ; w'_c is constant for $0 \leq \alpha_A/d \leq 1$, increases for $1 < \alpha_A/d \lesssim 5$, and attains a constant limit for $\alpha_A/d \rightarrow \infty$. (e) $\tau\beta_q$ as function of α_A/d for typical values of w_c , the black continuous lines correspond to Eq. (9) with β_{q_0} and β_{q_∞} listed in Table I. (f) q as function of α_A/d and $w_c = 0.0, 0.25, 0.5$; we verify that $q = 4/3, \forall 0 \leq \alpha_A/d < 1$, and is given by the expression which is indicated therein for $\alpha_A/d \geq 1$. These results remain as they stand for all values of τ .

geometrical problems. Such is the case of the Kasteleyn-Fortuin theorem [45], where the $q_{\text{Potts}} \rightarrow 1$ limit of the q_{Potts} -state Potts ferromagnet corresponds to bond percolation. That is also the case of the de Gennes isomorphism [46], where the $n \rightarrow 0$ limit of the n -vector ferromagnet corresponds to self-avoiding random walk, cornerstone of polymer physics. Our present numerical results suggest that analogous connections appear to exist between nonextensive statistical mechanical sys-

tems and (asymptotically) scale-free random networks.

ACKNOWLEDGEMENTS

We thank the High Performance Computing Center (NPAD/Universidade Federal do Rio Grande do Norte) for providing computational resources. Partial financial support from CNPq, Capes and Faperj (Brazilian agencies) is acknowledged as well.

[1] Oliver Mason and Mark Verwoerd, "Graph theory and networks in biology," *IET systems biology* **1**, 89–119 (2007).
[2] Stephen R Proulx, Daniel EL Promislow, and Patrick C Phillips, "Network thinking in ecology and evolution," *Trends in ecology & evolution* **20**, 345–353 (2005).
[3] Stanley Wasserman, Katherine Faust, *et al.*, "Social network analysis: Methods and applications," (1994).
[4] Stefano Boccaletti, Vito Latora, Yamir Moreno, Martin Chavez, and D-U Hwang, "Complex networks: Structure and dynamics," *Physics reports* **424**, 175–308 (2006).
[5] Pedro G Lind, Luciano R Da Silva, José S Andrade Jr, and Hans J Herrmann, "Spreading gossip in social networks," *Physical Review E* **76**, 036117 (2007).
[6] Tilch G., Ermakova T., and Fabian B., "A multilayer graph model of the internet topology," *International Journal of Networking and Virtual Organisations* **22**,

219–245 (2020).

[7] Brito S., Canabarro A., Chaves R., and Cavalcanti D., “Statistical properties of the quantum internet,” *Physical Review Letters* **124**, 210501 (2020).

[8] Newman M. E. J., “The structure of scientific collaboration networks,” *Proceedings of the national academy of sciences* **98**, 404–409 (2001).

[9] Mark EJ Newman, “Scientific collaboration networks. i. network construction and fundamental results,” *Physical review E* **64**, 016131 (2001).

[10] Danon L., Ford A. P., House T., Jewell C. P., Keeling M. J., Roberts G. O., Ross J. V., and Vernon M. C., “Networks and the epidemiology of infectious disease,” *Interdisciplinary perspectives on infectious diseases* **2011** (2011).

[11] Firth J. A., Hellewell J., Klepac P., Kissler S., Kucharski A. J., and Spurgin L. G., “Using a real-world network to model localized covid-19 control strategies,” *Nature medicine* **26**, 1616–1622 (2020).

[12] Sporns O., Tononi G., and Kötter R., “The human connectome: a structural description of the human brain,” *PLoS computational biology* **1**, e42 (2005).

[13] Mark EJ Newman, “The structure and function of complex networks,” *SIAM review* **45**, 167–256 (2003).

[14] Latora V. and Marchiori M., “Is the boston subway a small-world network?” *Physica A: Statistical Mechanics and its Applications* **314**, 109–113 (2002).

[15] Sporns O., “Network analysis, complexity, and brain function,” *Complexity* **8**, 56–60 (2002).

[16] Michael T Gastner and Mark EJ Newman, “The spatial structure of networks,” *The European Physical Journal B-Condensed Matter and Complex Systems* **49**, 247–252 (2006).

[17] Mark EJ Newman, “Analysis of weighted networks,” *Physical review E* **70**, 056131 (2004).

[18] Dorothy P Cheung and Mehmet Hadi Gunes, “A complex network analysis of the united states air transportation,” in *2012 IEEE/ACM International Conference on Advances in Social Networks Analysis and Mining* (IEEE, 2012) pp. 699–701.

[19] Alessandro Campa, Thierry Dauxois, Duccio Fanelli, and Stefano Ruffo, *Physics of long-range interacting systems* (OUP Oxford, 2014).

[20] Constantino Tsallis, “Possible generalization of boltzmann-gibbs statistics,” *Journal of statistical physics* **52**, 479–487 (1988).

[21] RM Pickup, R Cywinski, C Pappas, B Farago, and P Fouquet, “Generalized spin-glass relaxation,” *Physical review letters* **102**, 097202 (2009).

[22] G Livadiotis and DJ McComas, “Invariant kappa distribution in space plasmas out of equilibrium,” *The Astrophysical Journal* **741**, 88 (2011).

[23] Luis Carlos Malacarne, RS Mendes, and Ervin Kaminski Lenzi, “q-exponential distribution in urban agglomeration,” *Physical Review E* **65**, 017106 (2001).

[24] Shao-Zhen Lin, Peng-Cheng Chen, Liu-Yuan Guan, Yue Shao, Yu-Kun Hao, Qunyang Li, Bo Li, David A Weitz, and Xi-Qiao Feng, “Universal statistical laws for the velocities of collective migrating cells,” *Advanced Biosystems* **4**, 2000065 (2020).

[25] P Douglas, S Bergamini, and Ferruccio Renzoni, “Tunable tsallis distributions in dissipative optical lattices,” *Physical review letters* **96**, 110601 (2006).

[26] Eric Lutz and Ferruccio Renzoni, “Beyond boltzmann-gibbs statistical mechanics in optical lattices,” *Nature Physics* **9**, 615–619 (2013).

[27] Soares D. J. B., Tsallis C., Mariz A. M., and da Silva L. R., “Preferential attachment growth model and nonextensive statistical mechanics,” *EPL (Europhysics Letters)* **70**, 70 (2005).

[28] Brito S., da Silva L. R., and Tsallis C., “Role of dimensionality in complex networks,” *Scientific reports* **6**, 1–8 (2016).

[29] Nunes T. C., Brito S., da Silva L. R., and Tsallis C., “Role of dimensionality in preferential attachment growth in the bianconi–barabási model,” *Journal of Statistical Mechanics: Theory and Experiment* **2017**, 093402 (2017).

[30] Brito S., Nunes T. C., da Silva L. R., and Tsallis C., “Scaling properties of d-dimensional complex networks,” *Physical Review E* **99**, 012305 (2019).

[31] Cinardi N., Rapisarda A., and Tsallis C., “A generalised model for asymptotically-scale-free geographical networks,” *Journal of Statistical Mechanics: Theory and Experiment* **2020**, 043404 (2020).

[32] de Oliveira R. M., Brito S., da Silva L. R., and Tsallis C., “Connecting complex networks to nonadditive entropies,” *Scientific Reports* **11**, 1–7 (2021).

[33] Olivier Thas, *Comparing distributions*, Vol. 233 (Springer, 2010).

[34] Ian T Young, “Proof without prejudice: use of the kolmogorov-smirnov test for the analysis of histograms from flow systems and other sources,” *Journal of Histochemistry & Cytochemistry* **25**, 935–941 (1977).

[35] John A Peacock, “Two-dimensional goodness-of-fit testing in astronomy,” *Monthly Notices of the Royal Astronomical Society* **202**, 615–627 (1983).

[36] Swain M. J. and Ballard D. H., “Color indexing,” *International journal of computer vision* **7**, 11–32 (1991).

[37] Ming-Hsuan Yang, David J Kriegman, and Narendra Ahuja, “Detecting faces in images: A survey,” *IEEE Transactions on pattern analysis and machine intelligence* **24**, 34–58 (2002).

[38] Lauren E Wiesebron, John K Horne, Beth E Scott, and Benjamin J Williamson, “Comparing nekton distributions at two tidal energy sites suggests potential for generic environmental monitoring,” *International journal of marine energy* **16**, 235–249 (2016).

[39] Soon-Hyung Yook, Hawoong Jeong, A-L Barabási, and Yuhai Tu, “Weighted evolving networks,” *Physical review letters* **86**, 5835 (2001).

[40] Shijun Wang and Changshui Zhang, “Weighted competition scale-free network,” *Physical Review E* **70**, 066127 (2004).

[41] Marc Barthélémy, Alain Barrat, Romualdo Pastor-Satorras, and Alessandro Vespignani, “Characterization and modeling of weighted networks,” *Physica a: Statistical mechanics and its applications* **346**, 34–43 (2005).

[42] Luc Devroye, “Non-uniform random variate generation,” (Springer, New York, 1986).

[43] Harris C. R., Millman K. J., Van der Walt S. J., Gommers R., Virtanen P., D., et al., “Array programming with NumPy,” *Nature* **585**, 357–362 (2020).

- [44] Serfling R. J., *Approximation theorems of mathematical statistics*, Vol. 162 (John Wiley & Sons, 2009).
- [45] PW Kasteleyn and CM Fortuin, "Phase transitions in lattice systems with random local properties," *Physical Society of Japan Journal Supplement* **26**, 11 (1969).
- [46] Pierre-Gilles de Gennes, "Exponents for the excluded volume problem as derived by the wilson method," *Physics Letters A* **38**, 339–340 (1972).